DEPARTMENT OF ELECTRONICS AND
COMMUNICATION ENGINEERING
INDIAN INSTITUTE OF INFORMATION
TECHNOLOGY, DESIGN AND
MANUFACTURING KANCHEEPURAM
CHENNAI - 600127

*Synopsis Of*

# Self-Powered Flexible Thermoelectric Generator for Wearable Application

*A Thesis*

*To be submitted by*

**ANSHU PANBUDE**

*For the award of the degree*

*Of*

**DOCTOR OF PHILOSOPHY**

# 1    Abstract

Thermoelectric(TE) technology is an exceptionally promising method for directly converting thermal energy into electrical power. The TE technology is a green renewable energy technology. However, several factors are responsible for facilitating TE devices to offer low-cost electricity and sustainable energy technology without any mechanically moving components, including no harmful wastes that deteriorate environmental health. Even after achieving high performance, TE devices hinge on various factors, such as the properties of the material and the strategy employed for their applications in commercial sectors.

The substantial progress for readily available energy resources has put forth the biggest task of providing consistent and optimal power for various devices, from sensors to wearable applications. Already existing commercial thermoelectric generators (TEGs) are categorized as rigid bulk TEGs to eliminate the rigid components of a TEG. Firstly, the polyimide substrate replaces the ceramic substrate, and the polymer filler replaces the air gaps to achieve flexibility. In addition to replacing the copper electrode plate, a conductive metal-coated polyester fabric is utilized to attain a flexible interconnecting electrode structure. Lastly, the TE material in the bulk form is reduced to a thin film on cellulose fabric to represent a textile TEG, which represents a thin film. The performance analysis of the bulk and the thin film TEG is compared to better understand the future aspects of wearable technologies.

In the present work for the bulk flexible TEGs, we propose silicone elastomer as a compliant filling material for flexible thermoelectric generators (FTEG) with conductive fabric as electrodes interconnect for bismuth-telluride based thermoelectric legs, which permit TEGs to cover up curved surfaces. The use of texture profile analysis (TPA) to mechanically characterize the hardness, adhesiveness, springiness, resilience, cohesion ratio, and chewiness of silicone elastomer is performed. In addition, the statistically decreased adhesiveness and increased hardness, springiness, and chewiness identify silicone elastomer as a filling material for wearable thermoelectric devices. The ability of silicone elastomers to resist environmental effects such as water, moisture, heat, acid, alkali, corrosion, and weather aging is considered for wearable conditions.

As the demand for textiles in wearable electronics grows, researchers evaluate conductive textile materials distinguished by their blend of polyester and metal components. The electroplated nonwoven nickel copper conductive fabric has different compositions of nickel and copper on polyester. The structural and morphological properties of the conductive fabric are done for characterization studies to understand its behavior for further processes. The electrical conductivity of the conductive fabric is 0.05 S/cm$^2$. The average roughness of the electrode 0.191 $\mu$m provides the bonding adhesiveness. The Seebeck coefficient of 1.356 $\mu$V/K, the optimum concentration of charge carriers of the 3.46×10$^{19}$, the air permeability which allows the least thermal diffusivity of 0.08 mm$^2$/s obtained for the conductive fabric are appropriate for the thermoelectric power conversion. The elongation of 70 percent and the antimicrobial properties are among the other important aspects. The utility of conductive fabrics is expected to be an environment-friendly flexible fabric electrode in wearable thermoelectric applications.

The wearable, flexible thermoelectric generator is considered an auxiliary supply

to the battery for power generation to self-charge mode, which could generate electric potential from the human body and the environment. The FTEG is further studied for long-term reliability for electrical, mechanical, and thermal performance. The eight-leg FTEG in outdoor conditions at merely a 2 °C temperature gradient between the human body and the environment generates an output potential of 0.63 mV. The FTEG performance is also stable underwater to demonstrate weathering protection and can withstand 1300 bending cycles. The FTEG is also integrated with the voltage step-up converter to enhance the power generation without the help of any external source such as a capacitor or battery and illuminate an LED. The temperature sensitivity, mechanical strength, and ability to withstand the electrical parameters without significant changes make FTEGs exceptional wearable electronics.

Given the improvement in parameter ZT, i.e., thermoelectric efficiency, researchers are shifting towards 2-dimensional and 1-dimensional as well as 1-dimensional materials. In this work, we opt for 2-dimensional structures on conducting fabrics using the most widely used $Bi_2Te_3$ thermoelectric material to form the Pi ($\Pi$) and PN junction configuration. The 1D material fabrication as a TEG is crucial and incompatible with the TEG device architecture. $Bi_2Te_3$ thin films were successfully grown on cellulose fabrics using DC magnetron sputtering to overcome the challenges of the bulk thermoelectric generators. Structural, morphological, and thermoelectric properties of $Bi_2Te_3$ thin films have been investigated systematically to fabricate highly efficient thermal energy harvesting devices. The cellulose fabric is coated four times with the p type and n type $Bi_2Te_3$ thin film, and the study is done to observe the optimized thermoelectric device. X-ray diffraction data revealed that crystallites of $Bi_2Te_3$ films are highly oriented in plane with uniform distribution. Interestingly, the Seebeck coefficient (S) of the p type and n type $Bi_2Te_3$ thin film is 26.34 $\mu$V/K and -26.45 $\mu$V/K, respectively. Cellulose fabrics also display low thermal conductivity at room temperature and strongly favor achieving highly efficient thermoelectric generator devices for waste heat recovery and wearable applications. To find a potential TE material candidate to replace the toxic $Bi_2Te_3$, Graphite and its derivatives are studied for a thin film nanocomposite material coated on the cellulose fabric. Graphene and graphite derivatives can hold excellent mechanical properties, thermal assets, and optical, electronic, and excitonic possessions. Polyaniline (PANI) is the most versatile member of the class of Intrinsically Conducting Polymers (ICPs), and its ability to form a composite material with carbon-based nanostructured materials is studied for its significant properties. The highly conductive and flexible cellulose fabric is achieved by an easy two-step process, i.e., a blend of in-situ polymerization and solution techniques. These fabrics' elemental, morphological, structural, electrical, and thermal characteristics are studied. The electrical conductivity of the PANi/graphene composite fabrics improves over other coated fabrics. The thermopower value 0.045 $\mu$V/K of the PANi/graphene composite fabric is expected to be prominent for wearable thermoelectric devices. Along with the current scenario, we also tried to bring out some of the next steps that the researchers could take to overcome the challenges, enhance the power conversion, and improve the ZT of the flexible thermoelectric generators.

# 2 Objectives

Wearable thermoelectric power generators are among the most recent technological developments in small and portable electronics. Wearable thermoelectric generators (TEGs) measure the ambient temperature and the temperature of the human body to transform the temperature differential into electrical potential. When the ambient temperature changes, the temperature of the human body varies between 33 ℃ and 38 ℃. Furthermore, throughout the body's normal activity, the heat flow varies between 50 and 150 W/m$^2$ [1-7]. The performance of the thermoelectric device is determined by the thermoelectric figure of merit, ZT.

- Study of the Effectiveness of Conductive Fabrics as Electrode Interface

- Investigation of Encapsulating Materials for Flexible Thermoelectric Generation

- Self-powered Standalone Performance Study of Thermoelectric Generator for Body Heat Harvesting

- Fabrication of the thin film Pi and PN junction thermoelectric generator

- Incorporation of polyaniline on graphene-related materials for wearable thermoelectric applications

# 3 Existing Gaps Which Were Bridged

Commercial TEGs currently have a bulk and rigid structure and are not feasible for wearable applications. The TE leg matrix is unfilled, and for mechanical strength, encapsulation with rigid ceramic substrates is provided [8]. However, different filling materials can provide flexibility and mechanical strength and prevent the impacts of the environment and chemicals on the performance of thermoelectric generators. In the same series, to achieve flexible TEGs, the rigid copper electrode is also selected to be replaced by customized conductive fabrics. A conductive fabric is studied based on its electrical, thermoelectric, mechanical, and antimicrobial properties, which make it a considerable candidate for the electrode of the flexible thermoelectric generator. The main soul of the TEG is the thermoelectric material, and in the bulk devices, the TE legs are also rigid. When imagining a flexible TEG, the thermoelectric material could also be replaced as a thin film to acquire the desired flexibility. Consequently, to deal with this, a cellulose fabric is chosen for the substrate for thin film formation, and its performance is studied under various conditions. Achieving flexibility is not just the only goal of sustainable energy harvesting; the Bismuth Telluride could be replaced by incorporating polyaniline on graphene-related materials on cellulose fabrics for wearable thermoelectric applications [9-13].

# 4 Most Important Contributions

- Fabrication of TEG Model
  With the supposition of a flexible TEG, the conductive base electrode and the top electrode are customized as nickel-copper fabric. The pattern uses Autodesk

Fusion 360 and a laser-cut engraving design tool. The conductive fabric is cut with the assistance of a $CO_2$ laser cutting machine.
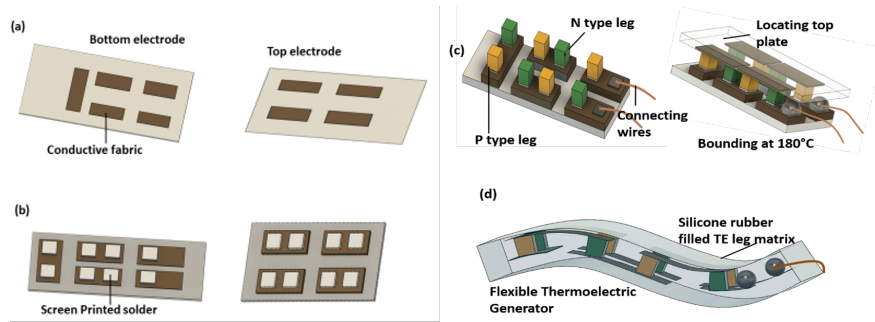


Figure 1: (a)-(d) Schematic representation of fabrication of FTEG
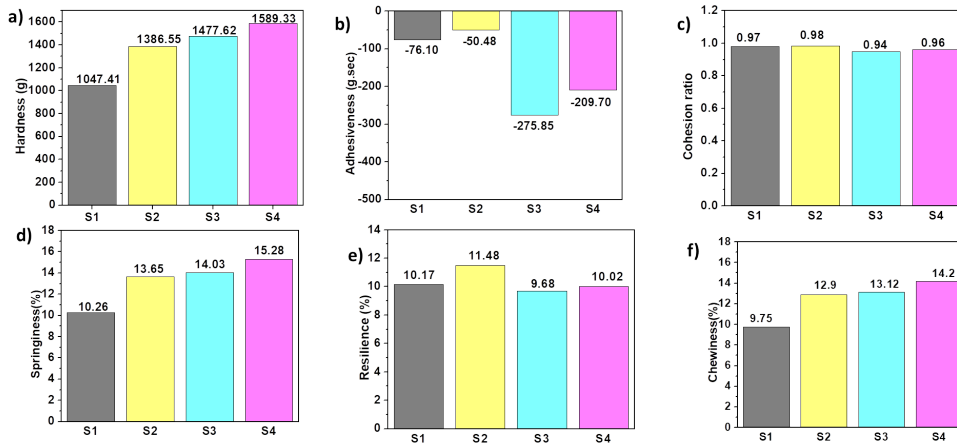


Figure 2: Texture Profile Analysis of silicone elastomer

Fig. 1 shows the detailed scheme of fabrication of FTEG. The designed conductive fabric is laser cut to obtain a Π-type structure between two substrates, as shown in Fig. 1(a). In Fig. 1(b), the solder paste is screen printed with the help of a stencil to provide an electrical bonding between the TE leg and the substrate. In addition, the substrate and the TE leg must be connected in series in electrical and parallel thermal connections, which calls for placing the thermoelectric legs in series order of p-n-p-n manner as demonstrated in Fig. 1(c). The connecting wires, the top and bottom substrate, are sandwiched and kept in a muffle furnace to bond the solder paste to the substrate and TE legs.

- Understanding of Silicone Elastomer as Filler Material
  Fig. 2 shows the texture profile analysis (TPA) of different silicone elastomers (S1, S2, S3, and S4) involved in the investigation as a filling material for a wearable thermoelectric generator. Fig. 2(a) shows the hardness of each sample. The crosslinking of the silicone resin with the platinum catalyst leaves no by-product. The vinyl/methyl bond of the polymer reacts with the addition-cured catalyst, forming a cross-linker molecule, and the catalyst becomes free to be available

for further crosslinking. So, the hardness of the S3 and S4 silicone elastomers was higher than that of S1 and S2, which are tin-based curings. Fig. 2(b) shows the minimum adhesiveness of S3 and S4, which refers to the energy required to separate the samples from the foreign materials and represents the extent of TEG conservancy compared to S1 and S2. Fig. 2(c) shows the cohesiveness of silicone elastomer samples, which measures the strength of internal linkages and the extent to which a material can be deformed before it ruptures. Fig. 2(d) shows the extent to which a product physically springs back after it has deformed during the first compression, defined as springiness. The high springiness is caused by the crosslinking process, which results in viscosity loss and a rise in modulus (storage). For S1 and S3, the viscosity is too high; in S2, the viscosity is low, comparatively to S4. Fig. 2(e) shows the enhanced cross-linking effectively blocks the molecular motion in the polymer matrix, reducing its distortion ability and thus reinforcing the polymer matrix to measure the resilience while being pulled under tensile load per unit volume before starting deformation. In Fig. 2(f), the polymerization of silicone elastomers strengthened the chewiness and resilience. For S4, high chewiness depicts the silicone's strength and elasticity, preventing the sample's damage. Effects of water, different solutions such as acid, alkali, and weathering effect of UV light on the silicone elastomer when treated for 72+ hours, and there is no major weight loss before and after, is illustrated in Table T2 with the percentage change in their weight.

Table 1: Chemical and UV Prevention

| Test | Before | After | % change in weight |
|------|--------|-------|--------------------|
| Water | 0.2075g | 0.2095g | 0.96 |
| Acid | 0.198g | 0.1602g | 19.09 |
| Alkali | 0.1747g | 0.1757g | 0.57 |
| UV exposure | 0.5852g | 0.5843g | 0.15 |

The silicone elastomer is exposed to UV for one hour for corrosion and weather-resistant testing. The test cycle was continuously repeated for 72 hours of UV irradiation. A negligible weight difference of 0.15% is detected after the UV exposure test.

- Studies of Nickel Copper Fabric as Conductive Base Electrode
  The Seebeck coefficient is crucial for the power factor calculation of the overall thermoelectric performance. It is discovered that the different Nickel Copper conductive fabrics(E1, E2, E3, and E4) have a Seebeck coefficient of 1.356 $\mu$V/K, which is almost identical to the Copper's Seebeck coefficient. The Seebeck coefficient value, which provides the fabric's strong conductivity, confirms that copper makes up a significant portion of the metal composition by weight. The carrier concentration of $10^{19}$ /cm$^3$ is the ideal value for thermoelectric applications, although higher concentrations of $10^{20}$ to $10^{23}$ /cm$^3$ show degenerate materials in a form compatible with metal materials in this scenario. The fabric's thermal

5

conductivity is reduced thanks to its air permeability. Higher thermal conductivity results from a low value for air permeability, and a higher thermal diffusivity accelerates heat spread, as shown in Fig. 3(a). According to measurements, the thermal diffusivity of the electrode sample selected for the electrode base is 0.57 $mm^2/s$.
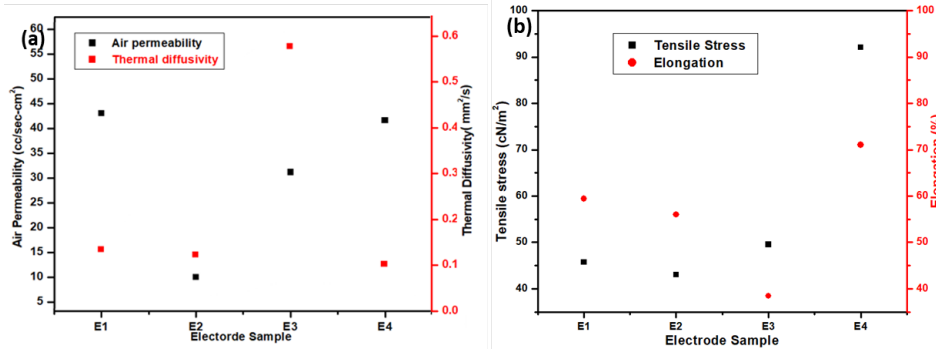


Figure 3: (a)Air permeability and thermal diffusivity, (b)Elongation and strength of conductive fabrics
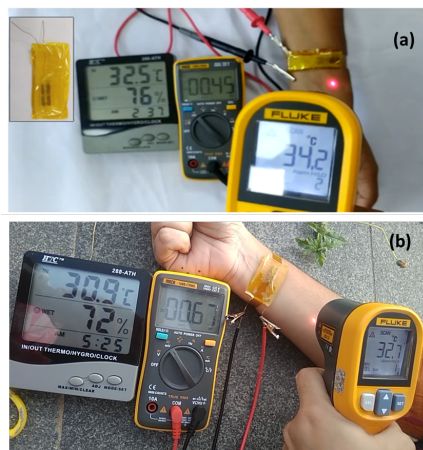


Figure 4: TEG Body Trials (a) Room ambiance (b) Outside environment

Creating elongated crystals of the nickel-copper structure on the polyester fabric increases the strength and flexibility of the fabric. It is evident that when surface roughness rises, shear strength also increases. Tensile stress increased from 45.78 $cN/m^2$ to 92.05 $cN/m^2$ for the electrode samples as shown in Fig 3(b) and the adhering surface roughness was 0.191 m for sample E4. The expansion of the bonding surface, the mechanical interaction between surface modification and adherent micro-columns, and other factors could be to blame for the increase in strength.

- Performance of The Free Standing Self Powered FTEG
  Fig. 4 represents the measurement of the electrical parameters to investigate the performance of the FTEG device for the potential generated from the human body. The inset image shows the fabricated FTEG of 2.4 cm x 3.9 cm. An

6
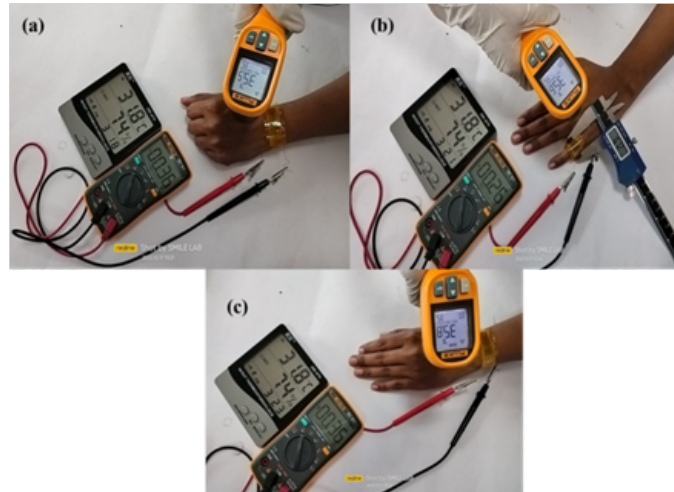
Figure 5: Bending of FTEG on finger and wrist
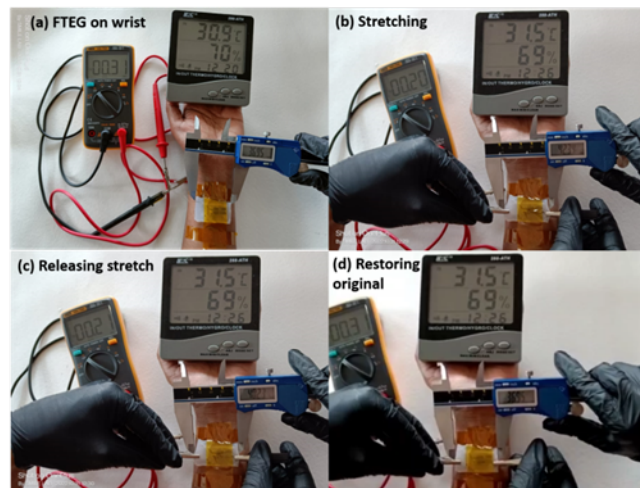


Figure 6: FTEG stretching before and after

ambient temperature on the top creates a temperature gradient with the human body temperature on the bottom side to generate a potential difference. Fig. 4(a) shows a temperature difference of 1.7 K and an open circuit voltage of 0.45 mV. Fig. 4(b) depicts 0.67 mV at a temperature gradient of 2 K for FTEG in outside environment conditions. The FTEG does not rely on any external power source.

- Analysis of the Mechanical Deformations of FTEG
  To analyze the changes in the FTEG sensing, we perform the bending test on the finger, and the potential is generated across the FTEG as shown in Fig. 5. With a temperature difference of around 4K, the FTEG is generating 0.26 mV, and the bending radius is 8.36 mm. The before and after bending also shows that at the same temperature difference, the potential generated by the FTEG is 0.36 mV. The FTEG is stretched from 36.95 mm to 42.34 mm and back to 36.95 mm, and even at a stretching of 14%, the FTEG senses the body temperature to generate voltage, as shown in Fig. 6. For the devices to function in a variety of hostile and demanding moistened conditions, stable wettability is desirable. The
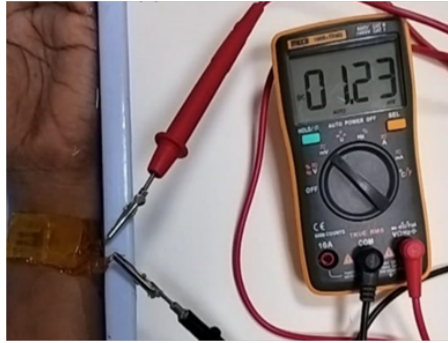
Figure 7: Potential generation by FTEG as submerged in water
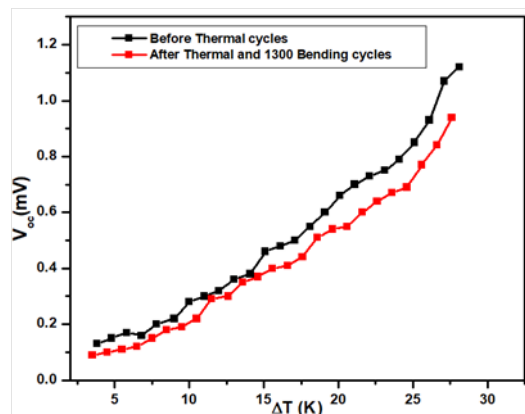


Figure 8: FTEG performance before and after 100 thermal cycles and 1300 bending cycles

polyimide tape, silicone elastomer, and conductive electrodes are water-resistant. As a result, when submerged in water, the FTEG on a human wrist creates a higher potential than at room temperature. The potential across FTEG is 1.23 mV, as shown in Fig. 7. For reliable operation under thermal cycling, the module's interface steadiness is essential. FTEG treated for 50 °C for 100 thermal cycles shows the FTEG output voltage is steady before and after thermal cycles, as well as the ability to withstand 1300 bending cycles, as shown in Fig. 8.

- Integration of The FTEG Array with The Voltage Step-up Converter
Fig. 9 shows that the series combination of 1 FTEG of 50 legs modules could power up an LED after integrating with a voltage step-up IC LTC3108. The minimum voltage requirement for the IC is 20 mV, and it could be configured with the FTEG array as a full-fledged wearable TEG module. Firstly, only one thermoelectric module is utilized in the prototype, and by increasing the number of thermoelectric modules, the voltage and power could be enhanced. The structural design and the heat sink assembly, along with the flexible substrate and reduction of the contact resistances, could improve the performance of FTEG.

- FTEG Coated on Cellulose Fabric
DC magnetron sputtering deposited n-$Bi_2Te_3$ and p-$Bi_2Te_3$ films. The FTEG device comprises six pairs of $Bi_2Te_3$ planar pattern to form the Pi ($\Pi$) and PN

8
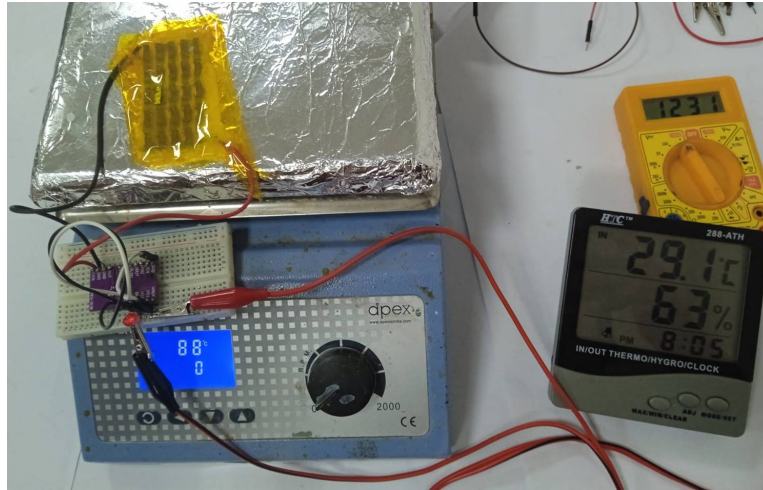
Figure 9: Integration of FTEG with voltage booster
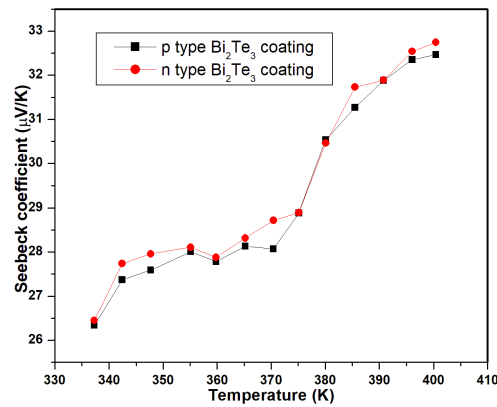


Figure 10: Seebeck coefficient of p-$Bi_2Te_3$ and n-$Bi_2Te_3$ thin film

junction thermoelectric device structure. Seebeck coefficient of n-$Bi_2Te_3$ and p-$Bi_2Te_3$ at room temperature is observed to be -26.34 $\mu$V/K and 26.45 $\mu$V/K, respectively. The variation of the Seebeck coefficient of the coated thin films at different temperatures is shown in Fig. 10, which shows the Seebeck coefficient of $Bi_2Te_3$ films as a function of the measured temperature. The increased S as the measuring temperature increased, resulting from the affected carrier density. The Hall measurement system measured the carrier concentration at room temperature, and the result shows the lower carrier concentration of p-type $Bi_2Te_3$ film 6.6 X $10^{10}$ /$cm^3$ and n-type $Bi_2Te_3$ thin film to be -2.7 X $10^9$ /$cm^3$. Fig. 11(a) shows the performance of $\Pi$ schematic TEG open circuit voltage 54.00 mV with a temperature gradient of 4 K where body temperature is 307 K and ambient temperature is 303 K in the indoor circumstances. In contrast, Fig. 11(b) shows the temperature gradient of 2.5 K harvest 41.9 mV for outdoor conditions. Fig. 12(a) shows that when the PN junction TEG is fixed on the human wrist with the temperature gradient at the room temperature of 3.2 K, it generates 89.8 mV. On

9

Figure 11: Wrist wearing Pi type FTEG a) Indoor ambiance b) Outdoor environment



Figure 12: Wrist wearing PN type FTEG a) Indoor ambiance b) Outdoor environment

the other hand, when the PN junction TEG is placed on the wrist in the outdoor environment and with a temperature gradient of 1.6 K, it generates 56.05 mV, as shown in Fig. 12(b). When a metal-semiconductor junction exists, there is always a situation that allows the flow of the electrons to be incorporated depending on the Fermi levels of both materials to match along with the direction of the flow of the electrons. The resistance appearing due to the flow of the electrons from the metal to the semiconductor interface leads to performance degradation if the thickness and the thin film dimensions are not optimized.

- Graphene Derivative Based TE Thin Film
PANi/Graphite coated on cellulose fabric is done using the solvothermal process. The XRD patterns captured for each coating applied to the cellulose cloth are displayed in Fig. 13(a). A distinctive broad PANi peak can be seen at roughly $23°\theta$. The PANi is grafted on GO, increasing the interlayer gap, where the bonding shift causes the matching peaks for the PGO composite fabric at $9°$ $\theta$ of (002) plane. Because of decreased crystallinity, the removal of oxygen groups from the GO surface, and the interaction of PANi with rGO, the PrGO plane at $25.8°\theta$ shows the plane shift. PANi, PGO, PrGO, and PG nanocomposites' average crystallite sizes are determined to be 5.64 nm, 4.68 nm, 20.176 nm, and 5.00 nm, respectively. To provide further comprehension, the samples are depicted by X-ray photoelectron spectroscopy, as shown in Fig 13(b). The PGO, PrGO, and PG specimen exhibits peaks for C 1s (at 281-283 eV), N 1s (at 398-400 eV), and O 1s (at 530-533 eV), indicating that C, O, and N make up the majority of the surface's
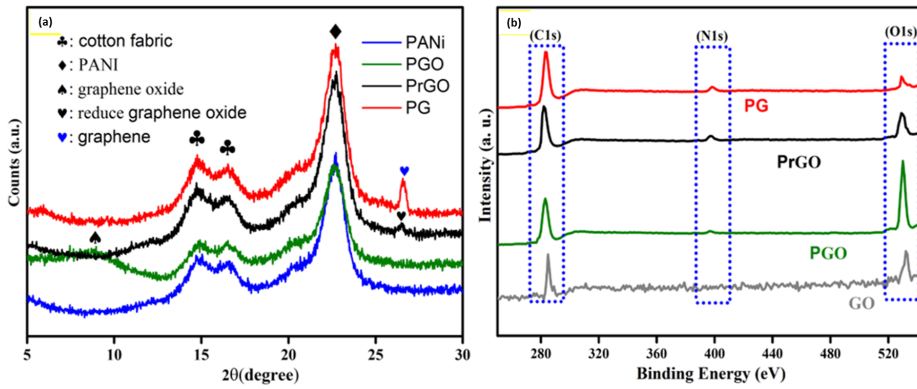
Figure 13: (a) XRD plot of PANi, PGO, PrGO, and PG. (b) XPS graph of GO, PGO, PrGO, and PG
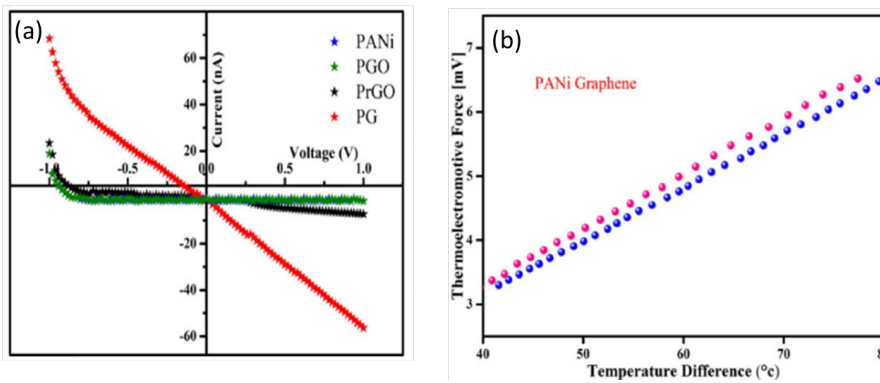


Figure 14: (a) I-V plot (b) Thermopower of PANi and Graphite derivatives coated cellulose fabric

elemental composition. The electrically conductive network is not supported by the PANi aggregated nanocomposites on the cellulose fabric in Fig. 14(a), which also displays high electrical resistivity. The electric network is built consistently, and the even distribution of PANi on the graphene-coated fabric gives the PG-coated cellulose fabric its linear curve and good conductivity. Fig 14(b) shows the thermopower of PG-coated cellulose fabric, which displays a linear relationship between temperature change and potential, and the positive slope shows the p-type material. It is discovered that the Seebeck coefficient is 85.5 $\mu$V/K. Hence, these materials are expected to be prominent for wearable thermoelectric devices.

# 5  Conclusions

In this work, the p-type $Bi_2Te_3$ and n-type $Bi_2Te_3$ TE devices have been investigated for characteristics, performance, and suitable wearable applications. Based on the research carried out, the report is structured into four major works: (a) Silicone elastomer as filling material in a TEG, (b) Flexible conductive Ni-Cu coated polyester fabric acting as interconnecting electrodes, (c) Fabrication and testing of $Bi_2Te_3$ Thin film TEG on cellulose fabric, (d) Polyaniline incorporated Graphite and its derivatives as ther-

11

moelectric material. The major findings from the work discussed in each chapter are summarized below: (a) The FTEG prepared using silicone elastomer as filling material is shown to overcome the limitations of rigid commercial thermoelectric generators. Our research shows that the silicone mixture ratio, curing duration, mold temperature, and their interactions are important factors for encapsulating or potting filler materials. (b) Flexible conductive electrodes made of fabrics with both the electrical and mechanical properties of fabrics are prepared to fabricate a well-defined flexible thermoelectric power generator. The customized electroplated nickel copper on polyester fabric was successfully shown to keep well adherent. (c) The hot plate experiment shows that extreme hot weather based on environmental temperature could generate higher voltages and power from the FTEGs and is very sensitive to temperature change. The FTEG bending effect on the internal resistance. The length of the FTEG decides the value of the bending radius and the FTEG encapsulation's thickness. The human body trials validated the FTEG's suitability for wearable applications. (d) We have studied thermoelectric transport properties of highly crystalline $Bi_2Te_3$ deposited films by DC magnetron sputtering for highly efficient thermal energy harvesting applications. Also, the $Bi_2Te_3$ coated on cellulose fabrics with n-type and p-type film at room temperature as a thermoelectric generator shows excellent performance at low-temperature gradients due to the reduction of the number of resistive contacts at the PN junction. (e) Lastly, PANi composite graphene nanoparticles were successfully grown on cellulose fabric using in-situ polymerization and then thoroughly examined. The PG-coated cellulose fabric exhibits consistent structural morphology with even distribution according to the diffraction patterns. Developing an electrically conductive network minimizes surface resistivity, highlighting the great improvement in the performance characteristics. These promising results suggest that the material fabrication on cellulose fabric can potentially be used for moderate waste heat harvesting for flexible wearable applications.

# 6 Organization of the Thesis

The proposed outline of the thesis is as follows:

Chapter 1: Introduction

Chapter 2: Literature Review

Chapter 3: Study of Cu-Ni Conductive Fabric as Electrode

Chapter 4: Investigation of Effect of Silicone Elastomer as Filling Material

Chapter 5: Performance Study of Flexible Thermoelectric Generator

Chapter 6: Fabrication of Thin Film Coated Pi and PN Junction Flexible Thermoelectric Generator

Chapter 7: Graphene Derivative Based Thermoelectric Thin Film

Chapter 8: Conclusion

# 7 List of Publications

Papers Published

1 Anshu Panbude, Pandiyarasan Veluswamy, "Silicone elastomer: Encapsulating Material for Flexible Thermoelectric Generator," IEEE Sensors Journal, vol. 23 (15), p. 16608-16615, Aug 2023, Impact factor- 4.325.

2 Anshu Panbude, Suhasini Sathiyamoorthy, R. Kumar, H. Shankar, S. Paulraje, V. Karthirvel, A.M. Adam, E.M.M. Ibrahim, K. Jayabal, Pandiyarasan Veluswamy, "Incorporation of Polyaniline on Graphene-Related Materials for Wearable Thermoelectric Applications," Material Letters, vol. 304(11), July 2021, Impact factor- 3.574.

Papers Submitted

1 Anshu Panbude, K Vivek Sai, Pandiyarasan Veluswamy, "Fabrication of Textile Based Thermoelectric Devices for Wearable Applications," Fibers and Polymers.

2 Anshu Panbude, Pandiyarasan Veluswamy, "Self-powered Standalone Performance of Thermoelectric Generator for Body Heat Harvesting" IEEE Sensors Letters.

3 Anshu Panbude, Pandiyarasan Veluswamy, "Effectiveness of Conductive Textiles as Electrode Interface to Enhance Power Conversion Efficiency for Wearable Applications," Solid States Sciences.

Other Publications

1 M. Subramani, L. Chandrasekar, Anshu Panbude, S. Sathiyamoorthy, Sivakami Mohandos, Pandiyarasan Veluswamy," Ultralow Thermal Conductivity Performance of Selenium-based Tetradymites via Solvothermal Assisted Annealing Method," Ceramics International, vol. 48(24), 2022, Impact factor- 5.53.

2 A.M. Adam, E.M.M. Ibrahim, Anshu Panbude, K. Jayabal, Pandiyarasan Veluswa -my, A.K. Diab, "Thermoelectric Power Properties of Ge Doped PbTe Alloys," Journal of Alloys and Compounds, vol. 872, 2021, Impact factor- 5.316.

3 T M Sivarenjini, Anshu Panbude, Suhasini Sathiyamoorthy, R Kumar, Malik Maaza, Jayabal K, and Pandiyarasan Veluswamy, "Design and Optimization of Flexible Thermoelectric Cooler for Wearable Applications," ECS Journal of Solid State Science and Technology, vol. 10(8), August 2021, Impact factor- 2.483.

Book chapter

1 Anshu Panbude, Pandiyarasan Veluswamy, Graphene-Based Materials for Thermoelectrics. In: Gupta, R. (eds) Handbook of Energy Materials. Springer, Singapore, July 2022.

Conference

1 Anshu Pannbude, Pandiyarasan Veluswamy. "Enhancing the performance parameter and adaptability of wearable, flexible thermoelectric generators using conductive textiles," 2023 $11^{th}$ International Conference on Nano and Materials Science (ICNMS2023), 13-15 January 2023.

2  Anshu Panbude, Pandiyarasan Veluswamy, "Photon Trapping by Fabric PIN for Hybrid Photo-Thermoelectric Energy Harvesting," The 7th Southeast Asia Conference on Thermoelectrics (SACT2022), December 2022.

3  Anshu Panbude, Pandiyarasan Veluswamy, "Enhancing the Conversion Effectiveness and Adaptability of Flexible Thermoelectric Generators for Sustainable Developments," International Conference On Emerging Materials for Sustainable Development (Emsd-2022), October 2022.

4  Anshu Panbude, Pandiyarasan Veluswamy, "Conductive Fabric based Silicone Encapsulated Flexible Thermoelectric Power Generation," 3rd Indian Materials Conclave and $32^{nd}$ Annual General Meeting of Materials Research Society of India (MRSI), Dec 2021.

# References

[1]  A.F.Ioffe, Semiconductor Thermoelements and Thermoelectric Cooling, Inforesearch Limited, London, p.103, 1956.

[2]  D.M. Rowe, Thermoelectrics Handbook Macro to Nano, CRC Press Taylor Francis Group LLC, p. 1008, 2006.

[3]  Xiaodong Wang, Zhiming M. Wang, Nanoscale Thermoelectrics, Springer International Publishing, Switzerland, p. 519, 2014.

[4]  Goldsmid, H.. "Bismuth Telluride And Its Alloys As Materials For Thermoelectric Generation," Materials, vol. 7(4), p. 2577-2592, 2014.

[5]  P. Dobnik, Woven Fabric Engineering, IntechOpen, 2010.

[6]  Xiaoming Tao, Wearable Electronics and Photonics, The Textile Institute: p. 81-104, WP, 2005.

[7]  Abu Raihan Mohammad Siddique et al., "A Review of the State of the Science on Wearable Thermoelectric Power Generators (TEGs) and their Existing Challenges," Renewable and Sustainable Energy Reviews, vol. 73, p. 730-744, 2017.

[8]  Zhong-Zhen Luo et al., "High Figure of Merit in Gallium-Doped Nanostructured n-Type PbTe-xGeTe with Midgap States," Journal of the American Chemical Society, vol. 141(40), p. 16169-16177, 2019.

[9]  Xiao-Lei Shi et al., "Advanced Thermoelectric Design: From Materials and Structures to Devices," Chem. Rev., vol. 120(15), p. 7399–7515, 2020.

[10]  Saeed Masoumi et al., "Organic-based Flexible Thermoelectric Generators: from Materials to Devices," Nano Energy, vol. 92, p. 106774, 2021.

[11] Hwanjoo Park et al., "High Power Output Based on Watch Strap-shaped Body Heat Harvester using Bulk Thermoelectric," Energy, vol. 187, p. 115935, 2019.

[12] Matteo Massetti et al., "Conventional Thermoelectric Materials for Energy Harvesting and Sensing Applications," Chem. Rev., vol. 121(20), p. 12465–12547, 2021.

[13] Xiang Li et al., "Recent Advances in Flexible Thermoelectric Films and Devices," Nano Energy, vol. 89, p. 106309, 2021.

[14] Y. Shi et al., "Design and Fabrication of Wearable Thermoelectric Generator Device for Heat Harvesting," IEEE Robotics and Automation Letters, vol. 3(1), p. 373-378, 2018.

[15] Nagaraj Nandihalli, "Thermoelectric Films and Periodic Structures and Spin Seebeck Effect Systems: Facets of Performance Optimization," Materials Today Energy, vol. 25, p. 100965, 2022.

[16] J. Choi, et al., "High-Performance, Wearable Thermoelectric Generator Based on a Highly Aligned Carbon Nanotube Sheet," ACS Appl. Energy Mater. , vol. 3, p. 1199  1206, 2020.

[17] M. Hyland et al., "Wearable Thermoelectric Generators for Human Body Heat Harvesting," Appl. Energy, vol. 182, p. 518-524, 2016.

[18] S. J. Kim, et al., "Post Ionized Defect Engineering of the Screen-Printed $Bi_2Te_{2.7}Se_{0.3}$ Thick Film for High Performance Flexible Thermoelectric Generator," Nano Energy, vol. 31, p. 258-263, 2017.

[19] Jin. Y. Oh et al., "Chemically Exfoliated Transition Metal Dichalcogenide Nanosheet-Based Wearable Thermoelectric Generators" Energy Environ. Sci. , vol. 9, p. 1696-1705. 2016.

[20] Nguyen Huu et al., "Flexible Thermoelectric Power Generator with Y-Type Structure Using Electrochemical Deposition Process," Appl. Energy, vol. 210, p. 467-476, 2018.

[21] Betty Lincoln, et al., "A Hybrid Ceramic-based Flexible Thermoelectric Nanogenerator with Enhanced Thermopower for Human Energy Harvesting," Energy Conversion and Management, vol 292, p. 117364, 2023.